CHAPTER 4

SOLID LIPID NANOPARTICLES IMPAIR AUTOPHAGIC FLUX IN PC3 PROSTATE CANCER CELLS: A NOVEL OPPORTUNITY FOR 'TARGETING' PROSTATE CANCER CELLS

MARCELO BISPO DE JESUS[1,2], VIOREL SIMION[3], CARMEN V. FERREIRA[2], DICK HOEKSTRA[1], INGE S. ZUHORN[1]

1. Department of Cell Biology, University of Groningen, University Medical Center Groningen, A. Deusinglaan 1, 9713 AV Groningen, The Netherlands
2. Department of Biochemistry, Institute of Biology, University of Campinas, UNICAMP, Campinas, SP, Brazil
3. Department of Biopathology and Therapy of Inflammation, Institute of Cellular Biology and Pathology "Nicolae Simionescu", Bucharest 050568, Romania

Submitted

Abstract. Gene therapy holds promise for reprograming cellular metabolism at the molecular level, thereby offering a potential cure for genetic diseases, including cancer. A variety of devices for cellular delivery of drugs and genes that more or less efficiently release their cargo into cells, has been developed and applied in recent years. Here we show that solid lipid nanoparticles (SLNs) composed of stearic acid, DOTAP, and pluronic F68, efficiently transfect malignant PC3 prostate cancer cells, but not non-malignant PNT2-C2 prostate cells. Interestingly, the specificity of this ability is emphasized by the notion that nanoparticles composed of lipofectamine transfect these cells with equal efficiency. Thus in case of lipofectamine-based devices, delivery of fluorescently-labeled ODNs, monitored by their accumulation into the nucleus, was fast and efficient in both cell types. However, although PC3 and noncancerous PNT2-C2 prostate cells internalize SLN lipoplexes with equal efficiency, SLNs displayed a slower but, eventually, similar efficiency compared to lipofectamine in case of delivery into PC3 cells, but very little if any nuclear delivery into noncancerous PNT2-C2 cells. Further investigations revealed that in both cell types SLN lipoplexes induce autophagosome formation, which is

connected with autophagic degradation in PNT2-C2 cells, but not in malignant PC3 cells. We suggest that a low autophagic flux in the PC3 tumor cells compared to that in non-malignant PNT2-C2 cells broadens the time window for effective endosomal escape of cargo, resulting in its selective and effective release into the tumor cells, but not their healthy counterparts. Accordingly, the application of SLNs provides a novel and 'selective' approach in the therapy of (prostate) cancer.

4.1 Introduction

CANCER can be caused by inherited or acquired genetic disorders that lead to uncontrolled cell proliferation [1]. A better understanding of the genetic mutations that lead to cancer and the development of protocols for gene expression modulation may lead to (personalized) cancer therapy [2]. As an alternative to conventional cancer treatments, commonly relying on the use of chemotherapeutics, the modulation of gene expression holds the promise to reprogram cancer cells at the molecular level and cure the disease [3].

Prostate cancer is a huge burden for human health, since it accounts for almost 30% of all diagnosed cases of cancer among men [4]. Annually, around 80,000 deaths are due to prostate cancer in Europe, while 190,000 new cases are diagnosed [5]. Treatment of prostate cancer may rely on surgery and/or radiotherapy and may be successful early after development of the disease but commonly fails when treatment initiates at later stages [5,6]. Thus, the design of new therapeutic approaches for prostate cancer treatment is highly desired.

Currently, an efficient gene delivery system stands between the theory and practice of gene therapy. Recently, solid lipid nanoparticles (SLNs) have attracted attention because of several physicochemical and pharmacological advantages over other delivery systems (e.g. liposomes and emulsions), such as a relative ease of large-scale production, superior physical stability, and long-term storage as lyophilized and sterilized formulations [7-10]. Furthermore, by inclusion of cationic lipids, SLNs hold promise as effective devices in gene and oligonucleotide delivery. For example, Jin et al. produced SLN formulations capable of efficiently delivering siRNA in the orthotopic glioblastoma xenograft model [11]. Jiang et al. used mannose-conjugated SLN formulations to target mannose receptors, and reported the successful transfection of Kupffer cells with high efficiency, both *in vitro* and *in vivo* [12].

Because cationic lipids were shown to induce the formation of autophagosomes [13], while autophagy has been implicated in the development of prostate cancer [14,15], we investigated the role of autophagy in SLN-mediated transfection of PNT2-C2 and PC3 cells.

Autophagy, or self-eating, is one of the major mechanisms for the degradation of cytoplasmic components, including misfolded proteins and damaged organelles [16]. Autophagy can also be triggered by nutrient starvation, allowing the cell to degrade proteins and organelles in order to 'recycle' nutrients [17]. During autophagy cytoplasmic components become engulfed in double membrane-bounded structures (autophagosomes) and are delivered to lysosomes/vacuoles for degradation [18,19]. During autophagosome formation, a cytosolic microtubule-associated protein light chain 3 (LC3) is processed and conjugated with phosphatidylethanolamine (PE) at its carboxyl terminus [20,21]. The PE-conjugated LC3, i.e., LC3- II, is inserted into autophagic vesicle membranes. Thus, LC3-II is widely considered as an autophagosomal marker [22,23]. The p62/SQSTM1 protein binds directly to LC3 II-positive vesicles and drive them for degradation in autophagosomes [24]. Therefore, changes in the p62 levels are inversely proportional to the autophagic flux [24].

Here, we show that SLNs colocalize with LC3 puncta in PNT2-C2 and PC3 cells, transfected with pLC3-GFP. Interestingly, p62 degradation, reflecting an increased autophagic flux, is only observed in PNT2-C2 cells. Because p62 degradation is negligible in PC3 cells, we conclude that a low autophagic flux in PC3 cells compared to PNT2-C2 cells, together with the slow endosomal escape of SLNs, results in efficient transfection of PC3, but not PNT2-C2 cells by SLNs. This mode of selective release of SLN contents in prostate cancer cells, but not in healthy counterparts may be exploited for SLN-based drug/gene therapy in prostate cancer.

4.2 Methods

4.2.1 Materials and Antibodies

Stearic acid (SA), Pluronic F68 (PLF68), and deoxyribonuclease I (DNase I) were purchased from Sigma-Aldrich (St. Louis, USA). The lipids N-[1-(2,3-Dioleoyloxy) propyl]-N,N,N-trimethyl-ammonium chloride (DOTAP), dioleoylphosphatidylethanolamine (DOPE), and 1,2-dioleoyl-sn-glycero-3-phosphoethanolamine-N-(lissamine rhodamine B sulfonyl) (Rhod-PE) were purchased from Avanti Polar Lipids (Alabaster, USA). Lipofectamine 2000® (LF2k) was from Invitrogen (Breda, The Netherlands), JetPEI was from Polyplus Transfection (NY, USA), and the plasmid pEGFP-N1 was purchased from BD Biosciences Clontech (Palo Alto, USA). Mouse anti-LAMP1 H4A3 was obtained from the Developmental Hybridoma Bank, University of Iowa, mouse anti-p62 clone D3 was obtained from Santa Cruz, mouse anti-beta-tubulin was obtained from Sigma (Zwijndrecht, The Netherlands) and mouse anti-early sorting endosome (EEA)1 from Abcam (Cambridge, United Kingdom). For immunostaining, secondary antibodies

(Alexa Fluor488, Alexa Fluor546) were purchased from Invitrogen. Cyto-ID® Autophagy Detection Kit was purchased from Enzo Life Sciences.

4.2.2 Preparation of SLNs

SLNs were prepared from a cationic microemulsion composed of SA (7 mM), DOTAP (1.25-2.5 mM), and PLF68 (1 mM), with or without DOPE (0.25-1.25 mM), using the microemulsion extrusion technique [25]. Briefly, SA was melted at 5-10 °C above its melting point under mechanic agitation, and dispersed into a hot aqueous solution of PL-F68 and DOTAP/DOPE. The hot solution was then passed 15 times through a polycarbonate membrane (100 nm pore size; Isopore™, Millipore) using a mini-extruder (Avanti Polar Lipids Inc., Alabaster, USA). Then, the suspension was cooled in a bath of 2 °C to prevent coalescence of the particles and was stored at 4 °C until further use. Fluorescently labeled SLNs were prepared by adding a trace amount of Rhod-PE (0.4 mol% relative to DOTAP/DOPE) into a hot aqueous solution of PL-F68 and DOTAP/DOPE.

4.2.3 Preparation of lipoplexes and polyplexes

Lipoplexes composed of SLNs and pEGFP-N1 (N/P 10:1) were prepared as follows: SLNs (2 μl) and pDNA (0.8 μg) were each diluted to an end volume of 50 μl in serum- and antibiotics-free medium. Subsequently, the solution containing the pDNA was added to the suspension containing the SLNs. The mixture (100 μl) was equilibrated for 20 min. at room temperature and used immediately after preparation. Lipoplexes composed of LF2k and pEGFP-N1 and polyplexes composed of JetPEI and pEGFP-N1 were prepared according to the manufacturer's protocol.

4.2.4 Cell culture, transfection protocol and cell association studies

PC3 and DU145 cells were obtained from the ATCC, and PNT2-C2 was kindly donated by N. Maitland, York. The PC3 prostate cancer cell line was maintained in Ham's F-12 nutrient mixture, Kaighn's modification (Sigma Chemical Co.), the DU145 cell line was maintained in MEM (Gibco), and the PNT2-C2 normal human prostate cell line was maintained in RPMI (RPMI)-1640 medium, supplemented with 2 mM glutamine. Mouse embryonic fibroblasts (MEF) Atg5 wild type [MEF-Atg5(+/+)], and Atg5 knockout [MEF-Atg5(-/-)] were a kind gift from Dr. Harm H. Kampinga (University Medical Center Groningen, Groningen, the Netherlands) and were maintained in DMEM medium. All media were supplemented with 10% (v/v) FCS, 100 U/mL penicillin and 100 μg/mL streptomycin. Cells were

grown at 37 °C under an atmosphere of 5% CO_2 in air and subcultured every 2 days using trypsin/EDTA. For transfection, cells were seeded on 12-well plates at a density that reached a confluency of 70-90% after 24 h. The cells were washed once with HBSS, and 400 μl of serum- and antibiotics-free medium was added per well. Next, 100 μl of lipo/polyplexes were added per well and incubated at 37°C. After 4h, the medium was replaced with complete medium. The percentage of EGFP-positive cells was determined after 24 h by means of flow cytometry (FACS/Calibur Flow Cytometer, Becton Dickinson, Mansfield, MA). To determine the total cell association of SLN lipoplexes, cells were incubated with lipoplexes, which were fluorescently labeled with 0.5 nmol of thioated TRITC–ODN (Biognostik, Germany). TRITC-positive cells were quantified after 30, 60, 120, and 240 min of incubation by flow cytometry (FACS/Calibur Flow Cytometer, Becton Dickinson, Mansfield, MA).

4.2.5 SLN internalization and transfection efficiency in the presence of endocytic pathway inhibitors

Cell plating conditions were the same as used for evaluating transfection efficiency, as described in the previous section. At the day of the experiment, the cells were washed once with HBSS and pre-treated with endocytic pathway inhibitors in medium for 30 min before adding the lipoplexes. To determine the total cell association of SLN lipoplexes, cells were incubated with SLN-lipoplexes, which were fluorescently labeled with a trace amount of Rhod-PE (0.4 mol%). After 4 hours, the fluorescence of extracellular lipoplexes was quenched using 0.2% trypan blue solution in HBSS (10 min, RT), and Rhod-PE-positive-cells were subsequently quantified by flow cytometry (FACS/Calibur Flow Cytometer, Becton Dickinson, Mansfield, MA). For determination of transfection efficiency, the cells were washed once with HBSS and pre-treated with endocytic pathway inhibitors in medium for 30 min before adding the lipoplexes. After 4 hours, the medium was aspirated and complete cell culture medium was added. After 24 hours, cells were collected by trypsination followed by centrifugation, and analyzed for GFP expression by flow cytometry (FACS/Calibur Flow Cytometer, Becton Dickinson, Mansfield, MA). Endocytic inhibitors were used at the following concentrations: 6 μg/ml chlorpromazine to inhibit clathrin mediated endocytosis (CME), 25 μg/ml nystatin to inhibit caveolar endocytosis, and 100 μM DMA (5-(N,N-dimethyl) amiloride hydrochloride) to inhibit macropinocytosis. Effective concentrations of the inhibitors were determined by measuring their effect on the uptake of markers for specific endocytic pathways by PC3 and PNT2-C2 cells, i.e., transferrin (5 min) for CME, cholera toxin B (30 min) for the caveolar pathway (data not shown). Cell viability of PNT2-C2 and PC3 cells was not compromised at the effective concentrations of the endocytic pathway inhibitors, as veri-

fied by an MTT assay (data not shown). Detection of autophagosomes and LC3-GFP puncta in transfected cells PNT2-C2 and PC3 cells were plated on coverslips and cultured overnight. Then, the cells were washed with HBSS and treated for 24h with lipoplexes/polyplexes, containing pEGFP-N1 that was labeled with Cy5 (LabelIT kit; Mirus Corporation, Madison, WI, USA). Subsequently, cells were stained for autophagosomes according to the manufacturer's instructions, using the Cyto-ID autophagy Detection Kit (Enzo Life Sciences, Farmingdale, USA), washed with HBSS, and fixed with 4% formaldehyde-PBS for 20 min. Coverslips were mounted onto glass slides with Prolong Gold Antifade reagent (Invitrogen, Carlsbad, CA). The samples were investigated using confocal microscopy (Leica TCS SP2 or Leica TCS SP8, Germany). To determine LC3 puncta formation, cells were transiently transfected with GFP-LC3 plasmid using Lipofectamine 2000. Afterwards, cells were treated for 4h with lipoplexes/polyplexes, containing Cy5 labeled pEGFP-N1 (LabelIT kit; Mirus Corporation, Madison, WI, USA). The samples were washed with HBSS and fixed with 4% formaldehyde-PBS for 20 min. Coverslips were mounted onto glass slides with Prolong Gold Antifade reagent (Invitrogen). The samples were analyzed for the presence of LC3-GFP puncta using confocal microscopy (Leica TCS SP2 and Leica TCS SP8, Germany).

4.2.6 Immunostaining for EEA-1 and LAMP-1 in PNT2-C2 and PC3 cells transfected with SLN lipoplexes

PC3 and PNT2-C2 cells were seeded 24 hours before the experiment at 1.5 10^5 cells/well on glass coverslips in a 12-wells plate. The next day, cells were incubated with fluorescently labeled SLNs for different times. After that, cells were washed with PBS, fixed for 20 min with 4% p-formaldehyde (PFA) in PBS, and the autofluorescence was quenched by 0.1 M glycin in PBS for 20 min. Then, cells were permeabilized with 0.2% triton X-100 for 2 min, and blocked with 10% serum solution in PBS for 5 min. Subsequently, cells were incubated with rabbit polyclonal anti-EEA1 (1:200) or anti-Lamp1 (1:200) for 1 h at 37 °C in a humid chamber. The primary antibodies were diluted in blocking solution. Cells were washed once with PBS and blocked for 1 min. Then, cells were incubated with Alexa Fluor-labeled secondary antibodies diluted 1:1000 in blocking solution, for 30 min at 37 °C in a humid chamber. After three times washing with PBS, coverslips were mounted on glass slides using Dako mounting medium (Dako, Carpinteria, USA). The samples were examined on a Leica TCS SP2 confocal microscope (Leica Microsystem, Germany) using a 63-oil-immersion lens. The images were acquired using the pinholes set to 1 airy unit for each channel at sequential manner and analyzed using ImageJ software (NIH).

4.2.7 Nuclear accumulation of FITC-labeled oligonucleotides in PNT2-C2 and PC3 cells incubated with SLN lipoplexes

SLN and LF2k lipoplexes, containing 0.5 nmol thioated FITC–ODN (Biognostik, Germany) were added to PNT2-C2 and PC3 cells, grown to 60–80% confluency in 12-well plates. After 30, 60, 120 and 240 min of incubation, cell nuclei were stained with DAPI. Several fields were randomly selected and about 10^4 cells were counted per condition. Images were taken using a TissueFAXS system equipped with a Zeiss AxioObserver Z1 microscope. The percentage of nuclei positive for FITC-ODN was quantified using DAPI-stained nuclei as 100% on the TissueQuest cell analysis software (TissueGnostics).

4.2.8 Quantification of p62/SQSTM1 in PC3 and PNT2-C2 cells incubated with SLN lipoplexes

Cells were transfected in 6 well plates as described above. Two, 4, and 8 h after transfection, cells were harvested, washed twice with PBS, and lysed on ice for 2 h in 200 μL of lysis buffer (50 mM Tris–HCl (pH 7.4), 150 mM NaCl, 1 mM EGTA, 20 mmol/L NaF, 1 mM Na3VO4, 0.25% sodium deoxycholate and protease inhibitors (1 μg/ml aprotinin, 10 μg/ml leupeptin, and 1 mM 4-(2-aminoethyl) benzenesulfonylfluoride hydrochloride). Protein concentrations were determined using the Bio-Rad protein assay, according to the manufacturer's instructions (Bio-Rad protein assay, Bio-Rad, Richmond, CA). An equal volume of 2 ×sodium dodecyl sulfate (SDS) gel loading buffer (100 mM Tris–HCl (pH 6.8), 200 mM DTT, 4% SDS, 0.1% bromophenol blue and 20% glycerol) was added to the samples which were subsequently boiled for 10 min at 100 ºC. Cellular proteins (20 μg) were resolved by SDS–polyacrylamide gel (12%) electrophoresis (PAGE) and transferred to PVDF membranes. After blocking for 1 h at room temperature with Odyssey™ blocking buffer, membranes were incubated simultaneously with primary antibodies (1:1000), for 1 h. Subsequently the incubation was continued with goat antirabbit 800 and goat antimouse 680 secondary antibodies (both at 1:20,000) for 45 min. After washing with physiological salt solution, the membranes were scanned using the Odyssey™ Infrared Imager. Actin or tubulin proteins were used as internal control. Autophagy was induced by nutrient starvation; cells were incubated with HBSS for 8 h and used as a positive control. In addition, cells were treated with bafilomycin A1 (200 nM), an inhibitor of autophagy, during nutrient starvation. These cells were processed for p62/SQSTM1 quantification as described above.

4.2.9 Statistical analysis

All experiments were performed in triplicate and were repeated independently at least three times. Means and standard deviations were calculated. An ANOVA test was performed to test for statistical significance ($p<0.05$) between the treatment groups.

4.3 Results

SLNs efficiently transfect PC3 prostate cancer cells but not non-cancerous PNT2-C2 prostate cells

Previously, we developed and characterized solid lipid nanoparticles (SLNs) composed of the fatty acid stearic acid (SA), the cationic lipid DOTAP, and the surfactant Pluronic F-68 for the delivery of genes into eukaryotic cells [26,27]. As shown in Fig. 4.1A, these SLNs effectively transfect prostate cancer cells with moderate (DU145) and high (PC3) metastatic potential, but, quite unexpectedly, not non-cancerous prostate cells (PNT2-C2). Thus, SLN transfection efficiency in PC3 and DU145 cells was 56.6 ±2.8% and 42.7 ±2.9%, respectively, whereas only 16.8 ±1.2% of the healthy PNT2-C2 prostate cells were transfected. Interestingly, however, the commercially available cationic lipid Lipofectamine 2000 (LF2k) efficiently transfects all three cell types to a similar extent, i.e., LF2k-mediated transfection efficiency in PC3, DU145, and PNT2-C2 cells was 55.0 ±1.7%, 68.5 ±15.9%, and 68.3 ±2.0%, respectively. Further experiments were performed to clarify the underlying mechanism for the preferential transfection of cancerous over non-cancerous prostate cells by SLNs. Evidently, such insight will be of help in developing improved strategies for SLN-mediated gene – and drug delivery into cells in general.

SLN lipoplexes associate to similar extents with PC3 and PNT2-C2 cells

Lipoplex-mediated nucleic acid delivery, or transfection, can be roughly divided into the following steps (i) cellular binding and uptake of lipoplexes, commonly by endocytosis; (ii) endosomal escape of nucleic acids; and (iii) -in case of DNA delivery- nuclear transfer, followed by transcription and translation. Therefore, it was first investigated whether differences in the efficiency of lipoplex-cell interaction could explain the observed differences in transfection efficiency. To this end, lipoplexes of SLNs and fluorescently labeled ODN were used to follow their cell-association kinetics with PC3 and PNT2-C2 cells. Fig. 4.1B shows that the overall efficiency of SLN-cell association, in terms of the percentage of cells involved, is fairly similar for both cell types. Furthermore, the net delivery of Rhod-PE labeled SLN lipoplexes in PC3 cells is approximately 1.5 -fold higher than in PNT2-C2

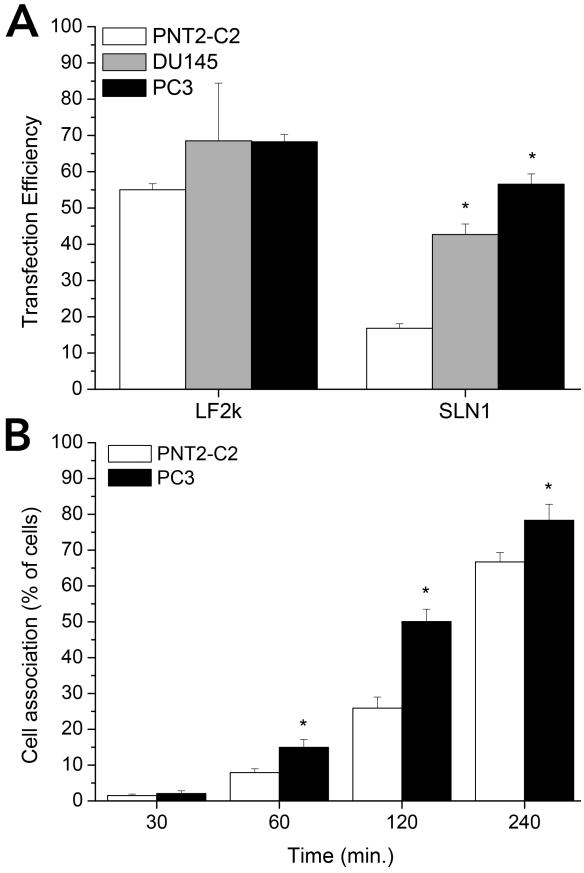

Figure 4.1. Transfection efficiency of LF2k and SLN lipoplexes in PNT2-C2, DU145 and PC3 cells. Cells were transfected with EGFP-encoding plasmid DNA using LF2k and SLN. The transfection was analyzed after 24 h by measuring EGFP positive cells by flow cytometry. Each value represents the mean ±S.D. of three independent experiments (n = 3). * $p<0.05$ - significant differences relative to transfection in PNT2-C2 cells (Dunnett's post-test). 1B. Internalization of fluorescently labeled SLN lipoplexes in PNT2-C2 and PC3 cells. SLNs complexed with TRITC labeled ODN were incubated with PC3 and PNT2-C2 cells at 37 °C. After each time interval (30, 60, 120 or 240 min), the percentage of cells positive for TRITC fluorescence was measured. Each value represents the mean ±S.D. (n = 8).

cells. Thus, after a 4 h of incubation the average fluorescence intensity in PC3 and PNT2-C2 cells was 221.4 ±59.4 and 145.4 ±32.1 (AU), respectively (data not shown). Because the difference in transfection efficiency

between PC3 and PNT2-C2 cells cannot be explained by differences in the efficiency of SLN-cell interaction, the next step in the transfection process, i.e., the endosomal escape, was therefore investigated.

Efficient endosomal escape of nucleic acids from SLN lipoplexes occurs in PC3 cells but not in PNT2-C2 cells

Typically, lipoplexes are internalized by cells via endocytosis [28,29], a process that, in principle, may transfer internalized material into lysosomes, where degradation may occur. Consequently, endosomal escape prior to transport into degradative lysosomes is an important parameter for the effective delivery of nucleic acids, and other biological therapeutic agents.

To determine whether SLNs promote endosomal escape of their cargo in PNT2-C2 and PC3 cells, cells were incubated with SLNs containing fluorescently labeled oligonucleotides (ODNs). ODNs rapidly (i.e., within approx. 5-10 min) accumulate in the cell nucleus following their release into the cytosol, and are therefore a useful tool to determine endosomal escape, as mediated by gene delivery systems [30]. Incubation of the cells with free ODNs led to negligible levels (< 5%) of positive nuclei in both PNT2-C2 and PC3 cells (Fig. 4.2A and B). This was expected, because free ODNs cannot destabilize the endosomal membrane, thus triggering their escape [31]. When ODNs were complexed with LF2k a very efficient and fast release from endosomes was observed in both cell lines. After 2, 4, and 6 h of incubation with LF2k lipoplexes, 26.3 ±5.8%, 66.4 ±16.3% and 66.6 ±10.4% of ODN-positive nuclei were detected in PNT2-C2 cells, respectively (Fig. 4.2A). In PC3 cells, 51.3 ±3.5% of ODN-positive nuclei were detected after 2 h, 75.5 ±6.3% after 4 h, and 83.3 ±8.5% after 6 h (Fig. 4.2B). In contrast, with SLN lipoplexes only 4.0 ±1.5% of the PNT2-C2 cells showed ODN-positive nuclei after 2 h, with a marginal increase up to 7.6 ±2.7% after 6 h of incubation (Fig. 4.2A). In PC3 cells, however, the percentage of positive nuclei, after an initial gradual increase from 4.4 ±1.6% after 2 h, to 23.7 ±5.3% after 4 h, reached a level of 59.3 ±10.1% after 6 h of incubation (Fig. 4.2B). These data reveal that compared to SLNs, LF2k mediates a relatively fast and efficient endosomal escape of ODNs, matching the levels of transfection efficiency obtained in both cell lines (cf. Fig. 4.1A). However, SLNs facilitate a slower, yet efficient endosomal escape of ODNs in PC3 cells, but little if any in case of non-cancerous PNT2-C2 cells. Similarly, also these data properly reflect the distinction seen in SLN-mediated transfection efficiency of PC3 cells versus PNT2-C2 cells, the latter being far less susceptible to transfection than the former (cf. Fig. 4.1A). Moreover, a similar parallel in differences of ODN release versus transfection efficiency can be drawn between the differences in efficiency seen for either delivery system as such, i.e., LF2k mediated endosomal releases is more efficient than that seen for SLNs, and concomitantly a higher trans-

fection efficiency is obtained. Together these data may imply that failure of efficient SLN-mediated destabilization of endosomal membranes in PNT2-C2 cells precludes effective transfection. Accordingly, in PNT2-C2 cells, the SLN lipoplexes might therefore be largely transported into degradative lysosomes, conditions that are of obvious disadvantage toward successful transfection. To better appreciate this possibility, further insight into the intracellular pathways of SLN processing in PC3 and PNT2-C2 cells was deemed necessary, which was examined next.

Internalization of SLN lipoplexes and transfection efficiency in the presence of metabolic inhibitors of endocytosis in PC3 and PNT2-C2 cells

The different endocytic pathways that are involved in the uptake of gene vectors, including clathrin-mediated endocytosis (CME), caveolae-mediated endocytosis (CvME), and macropinocytosis (MP), are connected to different intracellular fates. For example, cargo that is internalized via CME generally is transported into lysosomes, while in certain cell types cargo that is taken up via caveolae may not end up in lysosomes [32]. In addition, the rate of internalization and subsequent transport from early to late endosomes and lysosomes may differ among different routes of endocytosis. In general CME is connected to 'fast' and CvME to 'slow' endosomal processing [33]. To obtain insight into these processes in the present cellular systems, we therefore characterized the nature of the pathway(s) via which SLN lipoplexes delivered their cargo into PNT2-C2 and PC3 cells. Fluorescently labeled SLNs were used to monitor the internalization, i.e., after trypan-blue induced quenching of surface-bound Rhod-PE labeled SLNs (see Materials and Methods), in both cell lines in the absence and presence of the CME-inhibitor chlorpromazine (CPZ); the cholesterol-sequestering drug nystatin, that inhibits raft-dependent uptake, including CvME; the MP-inhibitor dimethylamiloride (DMA); and dynasore (Dy), a general blocker of dynamin-dependent endocytosis. As demonstrated in Fig. 4.3A, the internalization of SLN lipoplexes was severely impaired in both cell lines by dynasore, while it was not affected by nystatin. A remarkable distinction was seen when comparing the effect of the CME inhibitor, CPZ. While CME internalization of SLN in PNT2C2 cells was effectively inhibited, CPZ barely affected the internalization of SLN in PC3 cells. Remarkably, while the effect of CPZ on SLN-mediated transfection efficiency in PC3 cells is as expected, i.e., little if any effect on internalization and a virtually unaffected level of transfection, in PNT2-C2 cells the level of transfection efficiency was also unaffected in spite of the inhibition in internalization (Fig. 4.3A and B). This indicates that CME is not a productive route for SLN-mediated transfection. On the other hand, although NTT treatment did not significantly inhibit the internalization of

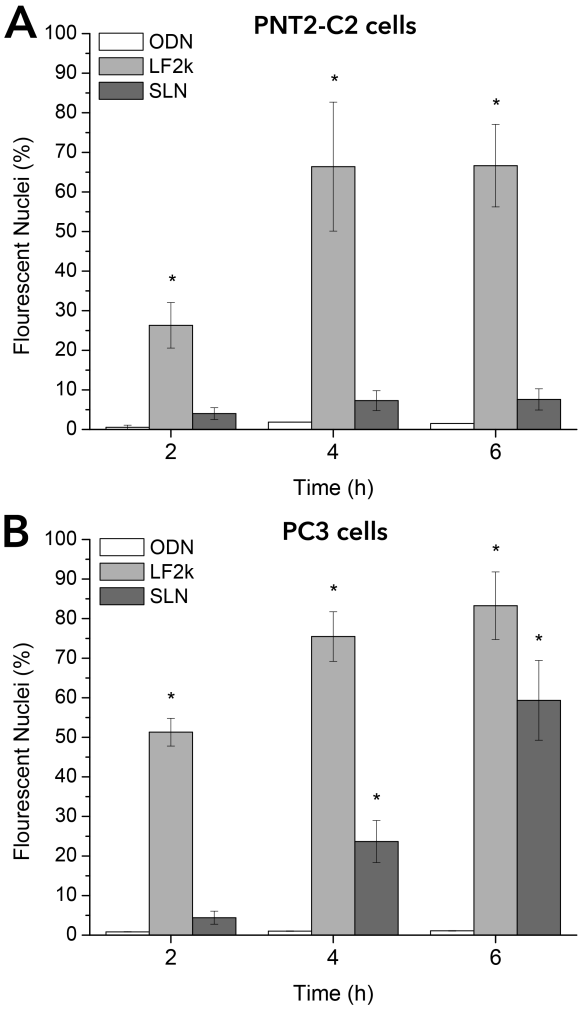

Figure 4.2. Endosomal escape of SLN lipoplexes in A) PNT2-C2 and B) PC3 cells. SLNs complexed with TRITC labeled ODN were incubated with PC3 and PNT2-C2 cells at 37 °C. After each time interval (2, 4, 6 h), the percentage of (DAPI-stained) nuclei that were positive for TRITC fluorescence was measured. Each value represents the mean ±S.D. (n = 3). * $p<0.05$ - significant differences relative to ODN group (Dunnett's post-test).

SLN lipoplexes, it did result in a drop in the transfection efficiency in both cell lines (Fig. 4.3B). In addition, transfection of PNT2-C2 cells was inhibited by dynasore, which suggests the involvement of (a) cholesterol-

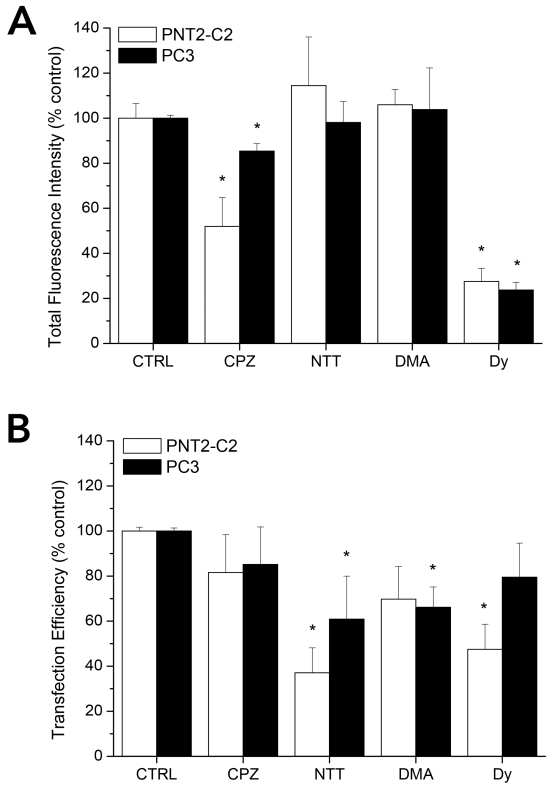

Figure 4.3. Internalization and transfection efficiency of PNT2-C2 and PC3 cells using SLN lipoplexes in the presence of endocytosis inhibitors. A) PNT2-C2 cells and PC3 cells were incubated with rhodamine-labeled SLN lipoplexes in the presence of endocytosis inhibitors, as detailed in Materials and Methods. After 4 h the total fluorescence intensity was analyzed. B) The transfection of PNT2-C2 cells and PC3 cells was analyzed after 24 h by measuring EGFP-positive cells by flow cytometry. Each value represents the mean ±S.D. of three independent experiments (n = 3). * $p<0.05$ - significant differences relative to internalization or transfection efficiency in absence of inhibitors (Dunnett's test).

and dynamin-dependent pathway(s) in transfection of PNT2-C2 by SLN. In PC3 cells, the transfection was almost unaffected by dynasore, while DMA caused a more pronounced inhibiton of transfection, suggesting that macropinocytosis significantly contributes to SLN transfection in PC3 cells (Fig. 4.3B). These results reveal key differences between the PC3 prostate cancer and non-cancerous PNT2-C2 prostate cells in how they may 'recog-

nize' and process the same device in a cell type-specific manner.

SLN lipoplexes end up in lysosomes in PC3 and PNT2-C2 cells

Further insight into the intracellular trafficking of SLN lipoplexes in PC3 prostate cancer cells and non-cancerous PNT2-C2 prostate cells were gained by confocal microscopy using fluorescently labeled SLN lipoplexes. First, the colocalization of Rhodamine-PE labeled SLN lipoplexes with early-endosomal autoantigen (EEA1) was evaluated. At an early stage, i.e., after 1h, SLN colocalizes with EEA1 in both cell lines (Fig. 4.4), indicating that endocytosis contributes to the pathway of entry of the SLN-based lipoplexes. After 8h of incubation with PNT2-C2 and PC3 cells, SLN lipoplexes clearly colocalize with LAMP-1, a late endosomal-lysosomal maker (Fig. 4.4). A slow endosomal release of oligonucleotides from SLN lipoplexes (cf. Fig. 4.2A) together with their processing into lysosomes where degradation of SLN prior to cytoplasmic release of the genetic cargo may occur, can explain the absence of significant transfection in PNT2-C2 cells. However, it does not explain the high transfection efficiency in PC3 cells, suggesting that in these cells, as opposed to PNT2-C2 cells, cargo release may occur prior to reaching the lysosomes (c.f. Fig. 4.2B) or, alternatively, that lysosomes in PC3 cells are less lytic, which would allow for a prolonged time window for cytosolic release of the genetic cargo from endo/lysosomes. However, we also considered autophagy as a possible mechanism by which intracellular delivered material, including nanocarriers, may become degraded, taking into account potential differences in tumor and non-tumorous cells.

SLN lipoplexes induce limited autophagic flux in PC3 cells compared to PNT2-C2 cells

Autophagy is one of the major mechanisms by which intracellular degradation occurs. Recently, it was reported that cationic gene vectors, specifically lipoplexes and polyplexes, induce autophagy in cells [13,34]. Moreover, autophagy and lysosomal malfunctioning have been suggested as potential mechanisms of nanoparticles toxicity [35]. Because autophagy has also been implicated to play a role in cancer development, it was of interest to investigate if PC3 prostate cancer cells and non-cancerous PNT2-C2 prostate cells show different autophagic responses to SLN lipoplexes, thus explaining potential differences in transfection efficiency (cf. Fig. 4.1A).

To investigate the autophagic response of PC3 and PNT2-C2 cells towards SLN lipoplexes, the induction of autophagosome formation upon addition of SLNs was analyzed, using a commercially available assay for autophagosome detection (Cyto-ID® Autophagy Detection Kit). An increase in the amount of autophagosomes was detected in PNT2-C2 and PC3 cells

Table 4.1. Autophagosome-positive cells in Control conditions, and after addition of SLN, LF2k lipoplexes and jetPEI polyplexes. (Autophagosome-positive cells: > 5 autophagosomes/cell)

	PNT2-C2	PC3
Control	44.5 ±7.5%	43 ±13.0%
LF2k	61.5 ±2.5%	73.5 ±0.5%
SLN	64.5 ±4.5%	69 ±3.0%
jet-PEI	87.5 ±7.5%	62.9 ±2.0%

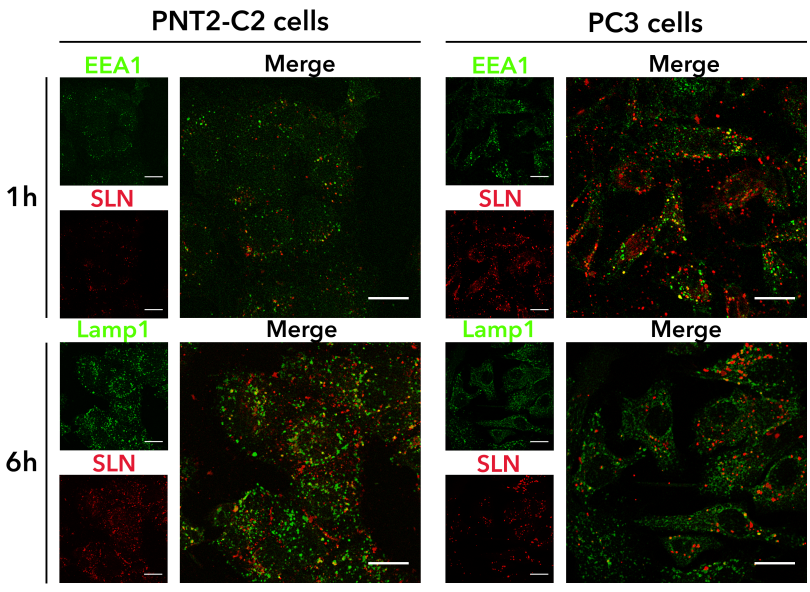

Figure 4.4. Intracellular localization of SLN in PNT2-C2 and PC3 cells. PNT2-C2 and PC3 cells were incubated with Rho-PE-labeled SLN lipoplexes. Colocalization of the SLN lipoplexes was determined with EEA1 (1 h) in PNT2-C2 cells and PC3 cells. Colocalization of the SLN lipoplexes was determined with Lamp1 (6 h) in PNT2-C2 cells and PC3 cells.

upon addition of SLN lipoplexes (Fig. 4.5 and Table 4.1), which indicates that SLN lipoplexes induce autophagosome formation in both cell types. A similar increase in autophagosome-positive cells was detected in both cell types following the addition of LF2k lipoplexes or another cationic gene vector, JetPEI polyplexes (Fig. 4.5 and Table 4.1).

To obtain further support and insight into the autophagy response in-

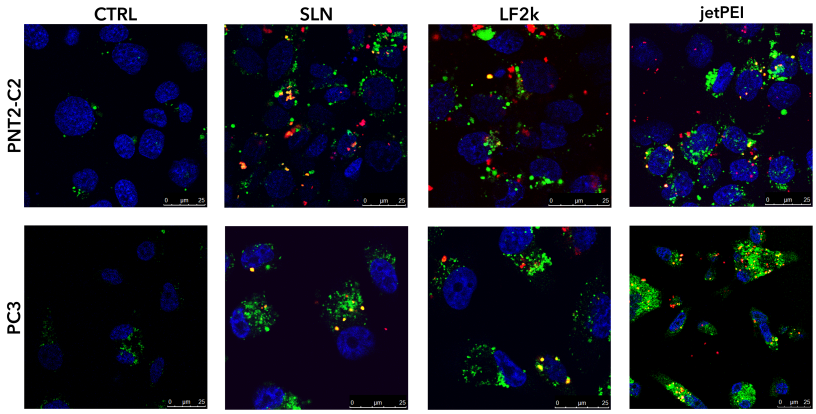

Figure 4.5. Induction of autophagosomes in PNT2-C2 and PC3 cells upon incubation with LF2k and SLN lipoplexes, and JetPEI polyplexes. PNT2-C2 and PC3 cells were incubated with SLN lipoplexes for 24 h and subsequently analyzed for the presence of autophagosomes using the Cyto-ID® Autophagy detection kit, as detailed in Materials and Methods. Green: Cyto-ID® labeled autophagosomes; red: Cy5-labeled lipo/polyplexes; blue: nuclei.

duced by SLN lipoplexes, PC3 and PNT2-C2 cells were transiently transfected with a GFP-tagged plasmid encoding LC3, a classic autophagy marker. 24h after transfection, the cells were incubated with Cy5-labeled SLN lipoplexes for 4h. As shown in Supplementary Fig. 4.8 the lipoplexes colocalize with GFP-LC3-marked autophagosomes in both cell lines. Consistently, also LF2k lipoplexes and JetPEI polyplexes colocalized with GFP-LC3 labeled autophagosomes, suggesting that after 4h the gene vectors may end up in autophagosomes, where they can be degraded (Supplementary Fig. 4.8).

To better appreciate a potential link between the transfection efficiency of SLNs and the autophagy machinery, SLN-mediated transfection was investigated in mouse embryonic fibroblasts with a functional (wt MEF ATG5+/+) and deficient (MEF ATG5-/-) autophagy machinery. The SLN transfection efficiency was significantly higher in ATG5-/- cells compared to ATG5+/+ cell line (Fig. 4.6). This effect was even more pronounced when using LF2k lipoplexes and JetPEI polyplexes (Fig. 4.6). The higher transfection efficiency in autophagy-deficient MEF ATG-/- cells compared to MEF ATG+/+ cells supports the notion that autophagy is involved in the processing of lipo/polyplexes in cells.

Whether the observed activation of autophagy facilitates actual degradation of the SLN lipoplexes, the autophagic flux, which is a measure for

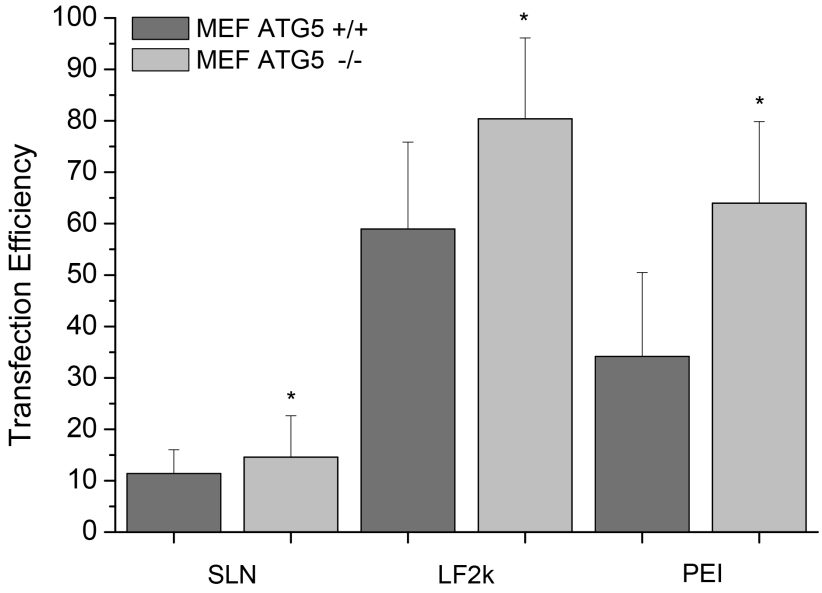

Figure 4.6. Transfection efficiency of SLN and LF2k lipoplexes and jetPEI polyplexes in autophagy-deficient MEF ATG5-/- and autophagy-proficient MEF ATG5+/+ cells. Cells were transfected with EGFP-encoding plasmid DNA using SLN, LF2k and jetPEI. The transfection was analyzed after 24 h by measuring EGPF positive cells by flow cytometry. Each value represents the mean ±S.E. of three independent experiments (n = 3). * $p<0.05$ - significant differences relative to transfection in MEF ATG5+/+ cells (student t-test).

the degradation of cargo 'ingested' by autophagosomes, was investigated by evaluation of the p62 levels. Because p62 accumulates when autophagy is inhibited, whereas decreased levels are observed when autophagy is induced, p62 is a useful marker for autophagic flux. Hence, PNT2-C2 and PC3 cells were incubated with SLN lipoplexes for 2, 4, and 8 h, and subsequently, the p62 levels were determined by immunoblotting. In PNT2-C2, the p62 protein level significantly decreased in a time-dependent manner (Fig. 4.7A, and quantification in Fig. 4.7B), indicating autophagic degradation. After 4h of incubation with SLN lipoplexes, the p62 level decreased to 64.9 ±1.0% of the control level, which further decreased to 34.2 ±0.1% after 8h of incubation. By contrast, in PC3 cells, the p62 levels remained constant over 8 h (Fig. 4.7A, and quantification in Fig. 4.7B). These data thus suggest that, although SLN lipoplexes induce autophagosome formation in both PNT2-C2 and PC3 cells (Table 4.1), autophagic degradation is

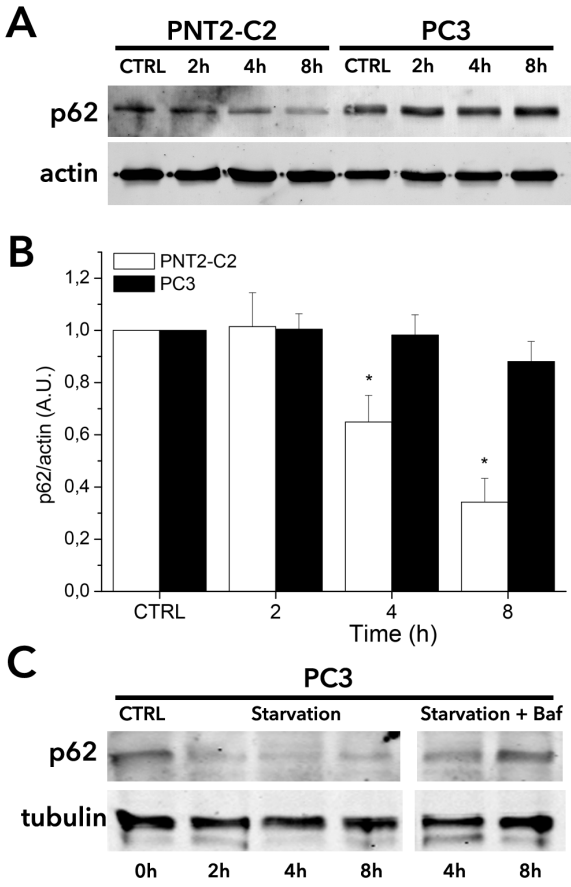

Figure 4.7. Autophagic flux in PNT2-C2 and PC3 cells treated with SLN lipoplexes. PNT2-C2 and PC3 cells were incubated with SLN lipoplexes for 2, 4, and 8h after which the p62 protein levels were detected by immunoblotting (A), and quantified by densitometry (B). In addition, the p62 protein level was determined in PC3 cells upon nutrient-starvation in the presence and absence of Bafilomycin A1 (C). The p62 levels were analyzed by western blot after 2, 4 and 8 h upon starvation.

only apparent in PNT2-C2 cells, and not in PC3 cells.

From these data it is unclear whether SLN lipoplexes impair autophagic flux in PC3 cells or that the limited autophagic degradation is a general hallmark of the PC3 cells. To investigate whether PC3 cells are able to induce autophagic degradation at all, the autophagic flux was measured in PC3 cells undergoing nutrient starvation, a strong inducer of autophagy.

The p62 western blot in Fig. 4.7C shows that p62 levels in PC3 cells decrease upon starvation, and that this decrease can be prevented by the autophagy inhibitor Bafilomycin A1, showing that degradation by autophagy is operational in PC3 cells. Interestingly, starvation-induced autophagy is known to be mTOR-dependent, whereas cationic lipids were shown to induce mTOR-independent autophagy [13]. It is therefore likely that in PC3 cells specifically this mTOR-independent autophagy is deregulated.

Altogether our data suggest that SLN lipoplexes induce a less efficient autophagic flux in PC3 cells than in non-cancerous PNT2-C2 cells. As a consequence, the degradation of SLN lipoplexes in PC3 cells is delayed/prevented, allowing a prolonged timespan for the cytosolic release of genetic cargo, leading to efficient transfection. Consistent with this notion are preliminary data (not shown), revealing the persistent presence of (fluorescently labeled) SLNs in PC3 cells after 24 h and their virtual absence in PNT2-C2 cells. However, whether SLN lipoplexes deliver their cargo via escape from endosomes, lysosomes, and/or autophagosomes remains to be determined. In normal PNT2-C2 prostate cells, that do show autophagic degradation upon the addition of gene vectors, the SLN lipoplexes are degraded prior to effective cargo release, resulting in low levels of transfection. Importantly, this divergence between the transfection of the two cell types only occurs when using a gene vector that presents a late endosomal escape, like SLN (Fig. 4.2). Gene vectors that show an early endosomal escape, like LF2k (Fig. 4.2), efficiently transfect both cell types, because they can induce endosomal escape prior to their degradation. Our finding that JetPEI, a polymer that shows late endosomal escape, because it is dependent on the drop in lumenal pH that typically occurs further down the endocytic pathway [30,36,37], efficiently transfects PC3 cells (47.69 ±3.33), and not PNT2-C2 cells (8.22 ±1.03), is in support of this finding.

4.4 Discussion

In this study we have demonstrated that SLN lipoplexes can efficiently transfect PC3 prostate cancer cells, but not normal PNT2-C2 prostate cells. A comparative analysis of the internalization pathway and intracellular processing of SLNs in PNT2-C2 and PC3 cells was performed to clarify the underlying mechanism for this difference.

A comparison of SLN internalization and transfection efficiency in the presence of endocytic inhibitors revealed that in PNT2-C2 cells transfection occurs via a cholesterol- and dynamin-dependent pathway, while in PC3 cells mainly macropinocytosis contributed to the cellular transfection. Nevertheless, irrespective of the routes of SLN internalization in PNT2-C2 and PC3 cells, SLN lipoplexes seem to end up in lysosomes in both cell lines. Interestingly, SLN-induced autophagy in the cells seems to contribute to ap-

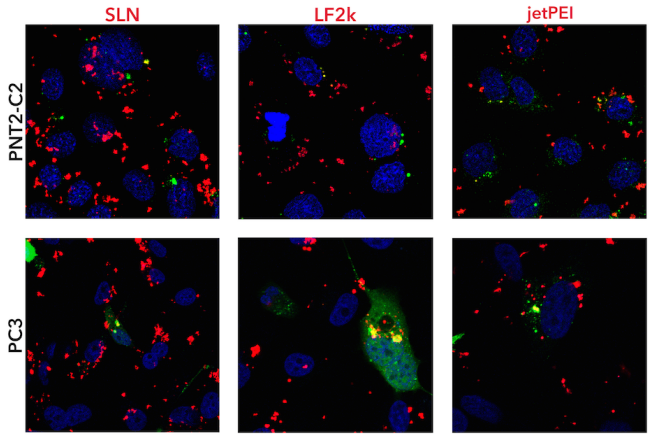

Supplementary Figure 4.8. Colocalization (indicated by white arrows) of LF2k and SLN lipoplexes, and JetPEI polyplexes with GFP-LC3 puncta in PNT2-C2 and PC3 cells. PNT2-C2 and PC3 cells were transiently transfected with pGFP-LC3 as detailed in Materials and Methods, then incubated with Cy5-labeled lipo/polyplexes for 4 hours. Green: GFP-LC3 puncta; red: Cy5-labeled lipo/polyplexes; blue: nuclei.

pearance of the delivery devices in this compartment, as was apparent from an increase in the number of autophagosomes in SLN-treated cells. While in PNT2-C2 cells the autophagic content becomes degraded, in PC3 cells the autophagic response does not result in degradation of the internalized material, as indicated by the unaltered p62 protein levels in the latter cell type. We reason that this lack of degradation allows an extended time window for release of the carrier's cargo into the cytosol and hence gene delivery by SLNs in PC3 cells when compared to PNT2-C2 cells, thus leading to the higher transfection efficiency in PC3 cells. The potency of SLN to transfect the cancer prostate PC3 cells rather than the normal prostate PNT2-C2 cells makes it an interesting vector for the treatment of prostate cancer by the ability to specifically accomplish cargo release of, for example, nucleic acid based drugs in tumor cells, while leaving normal cells 'unharmed'.

Several attempts were undertaken to interfere with the process of autophagy using widely used metabolic autophagy inhibitors, such as 3-methyladenine (3-MA) and Bafilomycin A1, and the autophagy activator rapamycin. However, because of a strong interconnection between endosomal and autophagosomal pathways [38] a direct effect of these compounds on the transfection process itself could not be excluded. For example, 3-MA may suppress endocytic fluid-phase uptake [39], and thus interfere

with early intracellular processing of the SLN lipoplexes. The autophagy inhibitor Bafilomycin A1 is known to prevent the endosomal acidification and thereby inhibit the endosomal escape by pH-responsive gene vectors, including PEI polymers. Therefore, this approach was not further pursued.

It is widely accepted that the non-targeted uptake of gene vectors can be highly efficient, while the intracellular trafficking of the vector together with the intrinsic properties of the vector, that regulate its endosomal escape, ultimately determine whether productive transfection will occur. Clearly, the intracellular sorting, trafficking, and fate of drug delivery vectors is influenced by (cancer) cell type [40]. Therefore, intrinsic differences in the cellular response toward nanocarriers between 'healthy' and 'malignant' cells can provide very interesting and promising opportunities for (cancer) cell-specific and thereby highly selective therapeutic intervention with genes, and other therapeutic agents.

Recently, a sophisticated polymer-peptide fusion was made, which is responsive to the increased PKCα activity that is typically observed in many types of cancer, and that shows cancer-specific gene expression [41]. In addition to the exploitation of an enhanced PKC activity, we show that in cancer cells impaired autophagy may provide an alternative means to 'passively' induce cancer-specific gene expression.

It will be of interest to investigate if the differential autophagic response in PC3 and PNT2-C2 cells is determined by the involvement of different uptake pathways that are involved in the intracellular processing of lipo- and polyplexes. For instance, if the impaired autophagic response is connected to the uptake of SLN via macropinocytosis, targeting of the vectors into the macropinocytic pathway may lead to further optimization of transfection efficiency. A thorough understanding of cancer cell signaling, especially upon interaction with (gene) vectors will aid in the rational design of drug delivery systems.

4.5 Acknowledgments

This research has benefited from the financial support of State of São Paulo Research Foundation (FAPESP) and Graduate School Drug Exploration (GUIDE). M.B.J. received fellowship from FAPESP (Proc. 2012/01038-9). V. S. obtained financial support from the European Social Fund PhD Programme POSDRU/107/1.5/S/ 82839.

4.6 References

[1] J.E. Visvader, Cells of origin in cancer, Nature. 469 (2011) 314–322. doi:10.1038/nature09781.
[2] J.E. Dancey, P.L. Bedard, N. Onetto, T.J. Hudson, The genetic

basis for cancer treatment decisions, Cell. 148 (2012) 409–420. doi:10.1016/j.cell.2012.01.014.
[3] H. Cao, R.S. Molday, J. Hu, Gene therapy: light is finally in the tunnel, Protein Cell. 2 (2011) 973–989. doi:10.1007/s13238-011-1126-y.
[4] R. Siegel, D. Naishadham, A. Jemal, Cancer statistics, 2013, CA Cancer J Clin. 63 (2013) 11–30. doi:10.3322/caac.21166.
[5] J.-E. Damber, G. Aus, Prostate cancer, Lancet. 371 (2008) 1710–1721. doi:10.1016/S0140-6736(08)60729-1.
[6] F. Labrie, Hormonal therapy of prostate cancer, Prog Brain Res. 182 (2010) 321–341. doi:10.1016/S0079-6123(10)82014-X.
[7] A. Dingler, S. Gohla, Production of solid lipid nanoparticles (SLN): scaling up feasibilities, J Microencapsul. 19 (2002) 11–16. doi:10.1080/02652040010018056.
[8] R. Parhi, P. Suresh, Preparation and characterization of solid lipid nanoparticles-a review, Curr Drug Discov Technol. 9 (2012) 2–16.
[9] A.A. Attama, SLN, NLC, LDC: State of the Art in Drug and Active Delivery, Recent Pat Drug Deliv Formul. 5 (2011) 178–187.
[10] S. Das, A. Chaudhury, Recent advances in lipid nanoparticle formulations with solid matrix for oral drug delivery, AAPS PharmSciTech. 12 (2011) 62–76. doi:10.1208/s12249-010-9563-0.
[11] J. Jin, K.H. Bae, H. Yang, S.J. Lee, H. Kim, Y. Kim, et al., In vivo specific delivery of c-Met siRNA to glioblastoma using cationic solid lipid nanoparticles, Bioconjug Chem. 22 (2011) 2568–2572. doi:10.1021/bc200406n.
[12] Z. Jiang, C. Sun, Z. Yin, F. Zhou, L. Ge, X. Liu, et al., Comparison of two kinds of nanomedicine for targeted gene therapy: premodified or postmodified gene delivery systems, Int J Nanomedicine. 7 (2012) 2019–2031. doi:10.2147/IJN.S30928.
[13] N. Man, Y. Chen, F. Zheng, W. Zhou, L.-P. Wen, Induction of genuine autophagy by cationic lipids in mammalian cells, Autophagy. 6 (2010).
[14] R.H. Kim, J.M. Coates, T.L. Bowles, G.P. McNerney, J. Sutcliffe, J.U. Jung, et al., Arginine deiminase as a novel therapy for prostate cancer induces autophagy and caspase-independent apoptosis, Cancer Res. 69 (2009) 700–708. doi:10.1158/0008-5472.CAN-08-3157.
[15] Z. Wu, P.-C. Chang, J.C. Yang, C.-Y. Chu, L.-Y. Wang, N.-T. Chen, et al., Autophagy Blockade Sensitizes Prostate Cancer Cells towards Src Family Kinase Inhibitors, Genes & Cancer. 1 (2010) 40–49. doi:10.1177/1947601909358324.
[16] Z. Yang, D.J. Klionsky, Eaten alive: a history of macroautophagy, Nat Cell Biol. 12 (2010) 814–822. doi:10.1038/ncb0910-814.
[17] B. Levine, D.J. Klionsky, Development by self-digestion: molecular mechanisms and biological functions of autophagy, Dev Cell. 6 (2004) 463–477.
[18] D.J. Klionsky, S.D. Emr, Autophagy as a regulated pathway of cellular degradation, Science. 290 (2000) 1717–1721.

[19] T. Yorimitsu, D.J. Klionsky, Autophagy: molecular machinery for self-eating, Cell Death Differ. 12 Suppl 2 (2005) 1542–1552. doi:10.1038/sj.cdd.4401765.
[20] Y. Kabeya, N. Mizushima, A. Yamamoto, S. Oshitani-Okamoto, Y. Ohsumi, T. Yoshimori, LC3, GABARAP and GATE16 localize to autophagosomal membrane depending on form-II formation, J Cell Sci. 117 (2004) 2805–2812. doi:10.1242/jcs.01131.
[21] Y. Ichimura, Y. Imamura, K. Emoto, M. Umeda, T. Noda, Y. Ohsumi, In vivo and in vitro reconstitution of Atg8 conjugation essential for autophagy, J Biol Chem. 279 (2004) 40584–40592. doi:10.1074/jbc.M405860200.
[22] N. Mizushima, T. Yoshimori, How to interpret LC3 immunoblotting, Autophagy. 3 (2007) 542–545.
[23] D.C. Rubinsztein, A.M. Cuervo, B. Ravikumar, S. Sarkar, V. Korolchuk, S. Kaushik, et al., In search of an "autophagomometer", Autophagy. 5 (2009) 585–589.
[24] S. Pankiv, T.H. Clausen, T. Lamark, A. Brech, J.-A. Bruun, H. Outzen, et al., p62/SQSTM1 binds directly to Atg8/LC3 to facilitate degradation of ubiquitinated protein aggregates by autophagy, J Biol Chem. 282 (2007) 24131–24145. doi:10.1074/jbc.M702824200.
[25] M.B. de Jesus, A. Radaic, I.S. Zuhorn, E. Paula, Microemulsion extrusion technique: a new method to produce lipid nanoparticles, J Nanopart Res. 15 (2013) 1–15.
[26] M.B. de Jesus, A. Radaic, W.L.J. Hinrichs, C.V. Ferreira, E. de Paula, D. Hoekstra, et al., Inclusion of the Helper Lipid Dioleoyl-Phosphatidylethanolamine in Solid Lipid Nanoparticles Inhibits Their Transfection Efficiency, J Biomed Nanotech. 10 (2014) 355–365. doi:10.1166/jbn.2014.1804.
[27] A. Radaic, E.D. Paula, M. Jesus, Factorial Design and Development of Solid Lipid Nanoparticles (SLN) for Gene Delivery, Journal of Nanoscience and .... (2015).
[28] I.S. Zuhorn, R. Kalicharan, D. Hoekstra, Lipoplex-mediated transfection of mammalian cells occurs through the cholesterol-dependent clathrin-mediated pathway of endocytosis, J Biol Chem. 277 (2002) 18021–18028. doi:10.1074/jbc.M111257200.
[29] J. Rejman, V. Oberle, I.S. Zuhorn, D. Hoekstra, Size-dependent internalization of particles via the pathways of clathrin- and caveolae-mediated endocytosis, Biochem J. 377 (2004) 159–169. doi:10.1042/BJ20031253.
[30] Z.U. Rehman, D. Hoekstra, I.S. Zuhorn, On the Mechanism of Polyplex- and Lipoplex-Mediated Delivery of Nucleic Acids: Real-Time Visualization of Transient Membrane Destabilization Without Endosomal Lysis, ACS Nano. (2013). doi:10.1021/nn3049494.
[31] I.S. Zuhorn, U. Bakowsky, E. Polushkin, W.H. Visser, M.C.A. Stuart, J.B.F.N. Engberts, et al., Nonbilayer phase of lipoplex-membrane mixture determines endosomal escape of genetic cargo and transfection efficiency,

Mol Ther. 11 (2005) 801–810. doi:10.1016/j.ymthe.2004.12.018.
[32] J. Rejman, M. Conese, D. Hoekstra, Gene transfer by means of lipo- and polyplexes: role of clathrin and caveolae-mediated endocytosis, J Liposome Res. 16 (2006) 237–247. doi:10.1080/08982100600848819.
[33] C. Beer, D.S. Andersen, A. Rojek, L. Pedersen, Caveola-dependent endocytic entry of amphotropic murine leukemia virus, J Virol. 79 (2005) 10776–10787. doi:10.1128/JVI.79.16.10776-10787.2005.
[34] R. Roberts, W.T. Al-Jamal, M. Whelband, P. Thomas, M. Jefferson, J. van den Bossche, et al., Autophagy and formation of tubulovesicular autophagosomes provide a barrier against nonviral gene delivery, Autophagy. 9 (2013) 667–682. doi:10.4161/auto.23877.
[35] S.T. Stern, P.P. Adiseshaiah, R.M. Crist, Autophagy and lysosomal dysfunction as emerging mechanisms of nanomaterial toxicity, Part Fibre Toxicol. 9 (2012) 20. doi:10.1186/1743-8977-9-20.
[36] A.K. Varkouhi, M. Scholte, G. Storm, H.J. Haisma, Endosomal escape pathways for delivery of biologicals, J Control Release. 151 (2011) 220–228. doi:10.1016/j.jconrel.2010.11.004.
[37] I.I. Canton, G.G. Battaglia, Endocytosis at the nanoscale, Chem Soc Rev. 41 (2012) 2718–2739. doi:10.1039/c2cs15309b.
[38] T. Hansen, T. Johansen, Following autophagy step by step, BMC Biol. 9 (2011) 39. doi:10.1371/journal.pone.0007124.
[39] P.E. Strømhaug, T.O. Berg, T. Gjøen, P.O. Seglen, Differences between fluid-phase endocytosis (pinocytosis) and receptor-mediated endocytosis in isolated rat hepatocytes, Eur J Cell Biol. 73 (1997) 28–39.
[40] S. Barua, K. Rege, Cancer-Cell-Phenotype-Dependent Differential Intracellular Trafficking of Unconjugated Quantum Dots, Small. 5 (2009) 370–376. doi:10.1002/smll.200800972.
[41] R. Toita, J.-H. Kang, T. Tomiyama, C.W. Kim, S. Shiosaki, T. Niidome, et al., Gene carrier showing all-or-none response to cancer cell signaling, J Am Chem Soc. 134 (2012) 15410–15417. doi:10.1021/ja305437n.